HHS Public Access

Author manuscript

Acc Chem Res. Author manuscript; available in PMC 2019 June 19.

Published in final edited form as:

Acc Chem Res. 2018 June 19; 51(6): 1465–1474. doi:10.1021/acs.accounts.8b00102.

Optothermal Manipulations of Colloidal Particles and Living Cells

Linhan Lin, **Eric H. Hill**, **Xiaolei Peng**, and **Yuebing Zheng***

Department of Mechanical Engineering and Texas Materials Institute, The University of Texas at Austin, Austin, TX 78712, USA

CONSPECTUS

Optical manipulation techniques are important in many fields. For instance, they enable bottom-up assembly of nanomaterials and high-resolution and *in-situ* analysis of biological cells and molecules, providing opportunities for discovery of new materials, medical diagnostics, and nanomedicines. Traditional optical tweezers have their applications limited due to the use of rigorous optics and high optical power. New strategies have been established for low-power optical manipulation techniques. Optothermal manipulation, which exploits photon-phonon conversion and matter migration under a light-controlled temperature gradient, is one of such emerging techniques. Elucidation of the underlying physics of opto-thermo-matter interaction and rational engineering of optical environments are required to realize diverse optothermal manipulation functionalities.

This account covers the working principles, design concepts and applications of a series of newly-developed optothermal manipulation techniques, including bubble-pen lithography, opto-thermophoretic tweezers, opto-thermoelectric tweezers, optothermal assembly, and opto-thermoelectric printing. In bubble-pen lithography, optical heating of a plasmonic substrate generates microbubbles at the solid-liquid interfaces to print diverse colloidal particles on the substrates. Programmable bubble printing of semiconductor quantum dots on different substrates and haptic control of printing have also been achieved. The key to optothermal tweezers is the ability to deliver colloidal particles from cold to hot regions of a temperature gradient, or a negative Soret effect. We explore different driving forces for the two types of optothermal tweezers. Opto-thermophoretic tweezers rely on an abnormal permittivity gradient built by structured solvent molecules in the electric double layer of colloidal particles and living cells in response to heat-induced entropy, and opto-thermoelectric tweezers exploit a thermophoresis-induced thermoelectric field for the low-power manipulation of small nanoparticles with minimum diameter around 20 nm. Furthermore, by incorporating depletion attraction into the optothermal tweezers system as particle-particle or particle-substrate binding force, we have achieved bottom-up assembly and reconfigurable optical printing of artificial colloidal matter. Beyond optothermal manipulation techniques in liquid environments, we also review recent progresses of gas-phase optothermal manipulation based on photophoresis. Photophoretic trapping and transport of light-

*Corresponding Author: zheng@austin.utexas.edu.

Notes

The authors declare no competing financial interest.

absorbing materials have been achieved through optical engineering to tune particle-molecule interactions during optical heating, and a novel optical trap display has been demonstrated.

An improved understanding of the colloidal response to temperature gradients will surely facilitate further innovations in optothermal manipulation. With their low-power operation, simple optics, and diverse functionalities, optothermal manipulation techniques will find a wide range of applications in life sciences, colloidal science, materials science and nanoscience, as well as in the developments of colloidal functional devices and nanomedicine.

Graphical Abstract

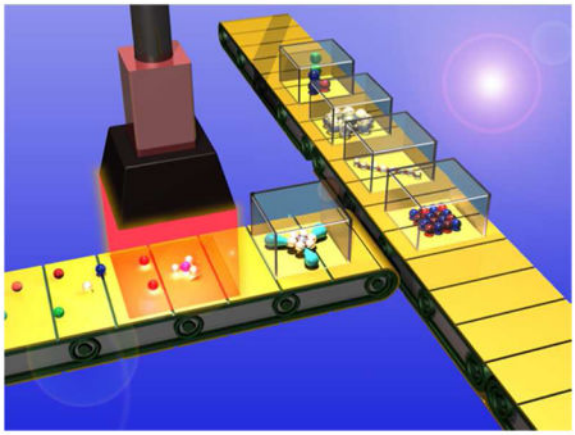

1. INTRODUCTION

Optical manipulation arises from direct or indirect light-matter interactions, which provide a light-directed driving force to deliver or trap colloidal particles. In optical tweezers, the deflection of incident light at the particle-environment interface generates an optical gradient force which can directly trap colloidal particles at the beam center.[1] Optical tweezers are versatile in manipulating a wide range of colloidal particles in three dimensions (3D).[2] The strength of the optical gradient force highly depends on the optical setup and the intensity of the trapping laser.[3] The working power of optical tweezers is generally high (10^2–10^3 mW), which could damage fragile objects such as biological cells.[4] Herein, we discuss several different strategies that were established to overcome the limitations of optical tweezers.

The excitation of localized surface plasmons at metal nanoantennas can significantly amplify the electromagnetic field in the vicinity of the nanoantennas, providing a plasmon-enhanced optical gradient force for near-field optical trapping, and thus reduce the operational power of plasmonic tweezers.[5] However, the localized nature of plasmonic hot spots limits the dynamic manipulation capability of plasmonic tweezers.[6] Another strategy is to introduce a light-controlled electric field or temperature field for indirect optical manipulation. For example, optoelectronic tweezers exploit the dielectrophoretic migration of particles under a light-controlled non-uniform electric field for low-power optical manipulation.[7] Optical manipulation through optical heating (i.e., optothermal tweezers) is alluring because photon-

phonon conversion is an entropically favorable process and heat-directed migration is widely applicable to variable particles in different fluidic environments.

Optothermal manipulation is a two-step process, i.e., photon-phonon conversion to optically build a temperature field and directed particle migration under the temperature field. The migration of colloidal particles under a temperature field involves multiple physical processes.[8–9] It has been shown that the migration of colloidal particles is sensitive to a variety of parameters such as the surface charge of the particles, solvent composition, environmental temperature and the morphology of the fluidic chamber, making it challenging to design a general optothermal platform for versatile colloidal manipulation.[10–11] Over the past twenty years, researchers have developed theories that describe the directed migration of colloidal particles within a temperature field.[12–15] Optothermal manipulation techniques for controlling colloidal particles under specific conditions have recently been demonstrated.[16–19]

This account summarizes recent progress in fundamental understanding, developments and applications of various optothermal manipulation techniques, including bubble-pen lithography, opto-thermophoretic tweezers, opto-thermoelectric tweezers, optothermal assembler, and opto-thermoelectric printing. In addition, photophoretic manipulation and its applications are discussed.

2. WORKING MECHANISMS OF OPTOTHERMAL MANIPULATION

Optothermal manipulation techniques introduced in this account are based on various opto-thermo-matter coupling phenomena such as Marangoni convention, thermophoresis, depletion interaction, thermoelectricity, and photophoresis, which are discussed in this section.

2.1. Marangoni convection

At the liquid-gas interface, the surface tension gradient $\nabla\gamma$ has the opposite sign as the temperature gradient, i.e., surface tension and temperature are inversely related. The surface tension gradient drives liquid migration from hot to cold region, as shown in Figure 1a. This convective flow provides a driving force to deliver colloidal particles in the liquid through Stokes' drag force, given by equation 2:

$$F_{\mathrm{d}} = 6\pi\eta R v \quad (2)$$

where η is the viscosity of the liquid, R is the mean radius of the particles, and v is the convective flow velocity.

2.2. Thermophoresis

Thermophoresis describes the directed migration of different components in the solution, including suspended colloidal particles, molecules, or micelles, along a temperature gradient.[20–22] Taking colloidal particles as an example, the drift velocity of the colloidal particles is given by:

$$u = -D_T \nabla T \quad (3)$$

where D_T is the thermophoretic mobility and ∇T is the temperature gradient. Since the Brownian diffusion coefficient D of different components in the solution has a difference of several orders of magnitude, the Soret coefficient $S_T = D_T/D$ is defined for a more general description of thermophoretic mobility (Figure 1b). The sign of S_T is a key parameter to achieve optothermal trapping of the colloidal particle at the laser beam.

2.3. Depletion Interaction

Depletion forces are common in hybrid systems, e.g., colloid-molecule mixtures.[16, 23] As shown in Figure 1c, both the depletants and colloidal particles can be driven by the temperature gradient. However, the small size of the molecules gives rise to a much larger Brownian diffusion coefficient, and the molecules migrate more quickly from the high-temperature to the low-temperature region, resulting in a concentration gradient ∇c once equilibrium is achieved. Osmotic pressure from the non-uniformly distributed molecules, which is proportional to ∇c, is exerted on a colloidal particle and drives the particle from cold to hot. Besides molecules, other materials such as nanoparticles, micelles, and vesicles, can act as the depletants to control the migration of colloidal particles.[24]

2.4. Thermoelectricity

In an electrolyte solution with an applied temperature gradient, ion diffusion occurs. Depending on ionic radius and solvation energy, ions are driven along the temperature gradient at different speeds or directions. In a steady state, the spatial separation between the cations and the anions generates a thermoelectric field, also known as the Seebeck effect:[14–15, 25–26]

$$E_T = \frac{k_B T \nabla T}{e} \frac{\sum_i Z_i n_i S_{Ti}}{\sum_i Z_i^2 n_i} \quad (4)$$

where i indicates the ionic species, k_B is the Boltzmann constant, T is the environmental temperature, e is the elemental charge, Z_i, n_i and S_{Ti} are the charge number, the concentration, and the Soret coefficient of ionic species i, respectively. As illustrated in Figure 1d, colloidal particles drifts along the thermoelectric field with a migration velocity v_P that is tunable by the dissolved ions.

2.5. Photophoresis

When a laser beam irradiates a light-absorbing particle, the asymmetric temperature distribution along the light propagation direction gives rise to an external force on the hot side of the particles from molecular interactions, e.g., air molecules at the hot side of the particle exert a larger force on the particle than at the cold side resulting in a net force towards the cold side (Fig. 1e).[27] Thus, photophoretic force can be either a pulling force or a

pushing force depending on the temperature distribution around the particles along the light propagation direction. However, in a liquid environment, the photophoretic effect can be much weaker due to the increased thermal conductivity compared with air.

3. OPTOTHERMAL MANIPULATION TECHNIQUES

3.1. Optothermal manipulation with microbubbles

Optical heating of a substrate immersed in liquid can generate microbubbles at the solid-liquid interface.[28–29] Zhao *et al.* demonstrated that optically generated microbubbles on a gold film can manipulate micron-sized polystyrene (PS) beads.[30] Microbubbles were also incorporated inside micro-machines to function as an optical syringe.[31] Use of a microbubble for optical manipulation relies on Marangoni convection induced by the stress tension gradient at the bubble surface to provide the force to drive colloidal particles toward the microbubble. The particles are trapped at the microbubble surface by the surface tension at the interface, which is balanced by the pressure difference between the gas in the bubble and the surrounding liquid.

We used optothermal microbubbles to print colloidal particles on substrates, which is termed bubble-pen lithography (BPL) (Figure 2).[32] The laser heating of a plasmonic substrate covered with a colloidal suspension generates a microbubble. The particles suspended in the solution are delivered to the bubble surface following a strong Marangoni convective flow (Figure 2b), trapped at the bubble/water interface, and eventually immobilized on the substrate due to van der Waals interactions. The size of the colloidal assemblies increases with the optical power of the laser due to the correlation between power and microbubble size. The lifetime of the bubbles is a function of the vapor composition inside the bubble and the bubble size. Without significant diffusion of air molecules into the bubbles, the lifetime of a sub-micron vapor bubble is about 100 ns, which is several orders of magnitude shorter than that of an air bubble (several seconds).[33] Taking advantage of the ultrashort lifetime of vapor bubbles, the on/off state of the bubble can be effectively controlled by the on/off state of the heating laser. By steering the laser beam in a colloidal suspension, we achieved continuous writing of assemblies of colloidal particles (Figure 2d) and selective printing of individual particles into arbitrary patterns (Figure 2e).

We have applied BPL to pattern colloidal particles of a wide range of sizes, shapes and compositions. Programmable patterning of semiconductor quantum dots was demonstrated at high resolution (~500 nm) and high throughput (10^4 μm/s).[34] The coupling between the quantum dots and the plasmonic substrate reduced their fluorescence lifetime (Figure 2f), which was tunable through controlling the optical power of the heating laser. Plasmonic layers were also incorporated into transition metal dichalcogenides and flexible substrates to enable BPL of colloidal particles, leading to heterogeneous materials and flexible devices (Figure 1g). We further interfaced BPL with a smartphone to achieve haptic operation (Figure 1h).[35]

Compared with other light-based printing techniques, (*e.g.*, optical printing of metallic nanoparticles using plasmon-enhanced radiation force[36–38] and UV-triggered click-chemistry using molecular reaction under UV light radiation[39]) BPL has shown its versality

in direct printing of low-dimensional objects of diverse sizes and materials without additional modification. However, BPL is limited by the high temperature required to generate vapor bubbles, and the printing of nanoscale colloids at single-particle resolution is currently not possible. The former can possibly damage fragile objects such as biological cells, while the latter can be potentially addressed through engineering of the substrate for generation of nano-sized bubbles.

3.2. Optothermal manipulation with thermophoresis

The challenge of thermophoretic manipulation lies in the uncertainty of the sign of Soret coefficient of particles in different solvent environments. The Soret coefficient of most colloidal particles and molecules has a positive value at or above room temperature in water.[11] Duhr *et al.* observed accumulation of DNA molecules at 3 °C and depletion of the molecules at room temperature.[17] The thermophobic nature of colloids at room temperature makes it difficult to employ thermophoresis for optical trapping because optical heating leads to diverged and bulk cooling regions. To overcome this obstacle, Braun *et al.* steered a heating laser along the circumference of a gold structure to create a localized and converged cooling region dynamically.[40–41] The heated gold structures acted as “hot walls” to drive the particle to the cooler central region for thermophoretic confinement. However, the confined particle underwent strong Brownian motion across a broad region, suggesting that the trapping stability is insufficient for dynamic tweezing. A recent study showed that micron-sized PS beads could be trapped *via* thermal convection and photophoresis through optical heating of amorphous Si.[19]

Opto-thermophoretic manipulation of high versatility relies on a negative Soret effect at or above room temperature. We proposed that interfacial entropy at the particle-water interface could drive the particle from cold to hot.[42] The thermophoretic mobility of a particle is given by equation 5.

$$D_{\mathrm{T}} = -\frac{\varepsilon}{2\eta T}\frac{2\Lambda_1}{2\Lambda_1+\Lambda_{\mathrm{p}}}\left(1+\frac{\partial \ln\varepsilon}{\partial \ln T}\right)\zeta^2 \quad (5)$$

where η is the solvent viscosity, ε is the solvent permittivity, T is the temperature, and Λ_1 and Λ_{p} are the thermal conductivities of the solvent and the particle, respectively. In bulk water, the permittivity-related term $\tau = \frac{\partial \ln\varepsilon}{\partial \ln T}$ has a value of −1.4 at room temperature, leading to a positive D_{T} and thus a thermophobic particle. However, in the electric double layer, the permittivity is quite different from the value of bulk water. As shown in Figure 3a, the polarized water molecules adsorb on the charged surface of the particle with specific orientation through electrostatic interaction. The permittivity of these structured water molecules is smaller than that of bulk water, leading to an abnormal permittivity gradient in the electric double layer with a positive τ value. Therefore, the particle migrates from cold to hot for trapping via optical heating. Above room temperature, the thermal perturbation of the structured water molecules increases the permittivity, reducing trapping stability. The trapping efficiency can be improved by increasing the surface charge of the particles or

reducing the ionic strength of the solution (Figure 3b). The proportional relationship between the in-plane trapping velocity v_T and the in-plane temperature gradient ∇T_r confirms the nature of thermophoretic migration. We further demonstrated parallel opto-themophoretic trapping of PS beads (Figure 3d).

We also realized the opto-thermophoretic manipulation of biological cells.[43] The bacterial membrane can be simplified as a bilayer composed of phospholipids with a hydrophilic headgroup and two hydrophobic fatty acid tails (Figure 4a). The cells themselves can be treated as charged particles which generate a localized electric field at the membrane surface. Water molecules adsorb on the membrane with specific orientation due to electrostatic interactions, with a permittivity gradient consistent with the temperature gradient in the electric double layer. We employed a digital micromirror device (DMD) to generate different optical images (Figure 4b) to enable versatile opto-thermophoretic manipulation of the cells with resolutions of 100 nm in distance and 1 degree in angle (Figure 4c).

Opto-thermophoretic tweezers have an operation power between traditional optical tweezers and optoelectronic tweezers,[7, 44] where the trapping force is not dictated by refractive index contrast between trapped objects and their environment. A further reduction of optical power is achieved through optimization of the substrate for improved optothermal convection efficiency. In addition, opto-thermophoretic trapping in a solvent with high ionic strength, which is important for biological applications, has not yet been achieved.

3.3. Optothermal manipulation with thermoelectricity

Thermoelectric fields have proven effective for optothermal manipulation of colloidal particles,[14] micelles,[25] and charged molecules.[15] Based on the Soret coefficients of three ions, i.e., S_T (OH^-) > S_T (Na^+) > S_T (Cl^-), one can predict that a negatively charged particle migrates from cold to hot in NaOH solution and from hot to cold in NaCl solution.[15] However, to trap different colloidal particles with opposite surface charge in the same salt solution is challenging because of the opposite signs of Soret coefficients.

We addressed this challenge by use of the cationic surfactant cetyltrimethylammonium chloride (CTAC, see Figure 5a). The CTAC surfactant coats the colloidal particles through hydrophobic and electrostatic interactions, leading to a hydrophilic, positively-charged surface. Meanwhile, CTAC self-assembles into cationic micelles above its critical micelle concentration (0.13–0.16 mM), which serve as positive “macro-ions” to generate a thermoelectric field in concert with the Cl^- counterions. Both CTAC micelles and Cl^- ions undergo thermophoresis from hot to cold regions with S_T (micelle) > S_T (Cl^-) and builds a thermoelectric field, which delivers the positively-charged particle from cold to hot to be trapped by the laser beam (Figure 5b).[45] When the particle is trapped in the vicinity of the substrate, the excluded micellar volume from the particle-substrate gap gives rise to the depletion attraction force to further confine the particle. A minimum trapping stiffness occurs at a CTAC concentration of 1–2 mM (Figure 5c). At 20 mM CTAC, the trapping potential depth of a single 100 nm silver nanosphere (AgNS) at a low optical power of 0.4 mW reaches 48 k_BT (Figure 5d), with the corresponding trapping force of 380 fN (Figure 5e). We further analyzed the trapped particles *via* dark-field scattering spectroscopy to

identify the size, shape, and material of the particles (Figure 5f). It should be noted that when metallic nanoparticles are trapped and heated by a laser beam, the particles undergo "hot Brownian motion" which can be analytically described by the temperature profile and the temperature-dependent viscosity profile,[46] giving rise to another power-dependent term besides the confinement of the thermoelectric field and depletion interaction.

With DMD-based light control, we achieved parallel opto-thermoelectric trapping of multiple metal nanoparticles (Figure 6a).[45] Multiple metal nanoparticles can also be assembled under a single laser beam spot.[47] Interestingly, the metal nanoparticle assembly can also act as a plasmonic heating source, which provides a temperature field for directing particle assembly over non-plasmonic substrates (Figures 6b and 6c). Due to the inter-particle plasmonic coupling, assemblies of metal nanoparticles are promising for *in-situ* analysis of target molecules in their liquid environments using surface-enhanced Raman spectroscopy (SERS). Tuning the inter-particle interactions and assembly size (Figure 6d) enabled a detection limit of 1 μM for rhodamine 6G using the AgNS assemblies (Figure 6e).

We have further demonstrated the optothermal assembly of colloidal matter with precisely controlled configurations (Figure 7a) by using CTAC micelles as depletants.[48] Upon optical heating, thermophoresis depletes CTAC micelles at the inter-particle gap with a depletion volume $V_{\mathrm{EV}}^{\mathrm{pp}}(r)$ and an osmotic pressure difference $\Delta\Pi$.[49] Considering the depletion force $F_{\mathrm{d}} = -\Delta\Pi V_{\mathrm{EV}}^{\mathrm{pp}}(r)$, the van der Waals force F_{vdw} and electrostatic interaction force F_{e}, we calculated the total interaction potential between two connected particles. Interestingly, the adhesion strength and interparticle distance are tunable by the CTAC concentration (Figure 7b). Bonding between the colloidal particles can be maintained when the temperature field is removed once the total potential well exceeds several $k_{\mathrm{B}}T$. Based on this understanding, we have assembled colloidal matter of different configurations from various colloidal particles (Figure 7c).

Finally, reconfigurable opto-thermoelectric printing of colloidal particles on substrates was achieved by exploiting the electrostatic repulsive interaction between the CTAC micelles and the CTAC-coated particles.[50] NaCl is added to the solution to create a trapping thermoelectric field, under which the cationic CTAC micelles are accumulated at the laser spot and create another repelling electric field pointing to the cold region (Figure 8a). The migration of charged particles along the temperature gradient depends on the exchange between these two electric fields. We have built a phase diagram that shows different particle-manipulation regimes when salt concentration and optical power are tuned (Figure 8b). At an optimized NaCl concentration between 20 and 30 mM, an increase of optical power leads to the transition from trapping to printing, where the particle-substrate depletion attraction force binds the particle onto the substrate (Figure 8c). The opto-thermoelectric printing of PS beads into different patterns were demonstrated (Figure 8d). To detach a printed particle from the substrate, the laser beam is centered on the particle to drive the CTAC micelles into the particle-substrate gap, and the accumulated CTAC micelles break the particle-substrate adhesion to release the particle. The erasing and reprinting of PS beads are demonstrated in Figure 8e.

An optical intensity three orders of magnitudes lower than optical tweezers allows opto-thermoelectric tweezers to operate with significantly reduced thermal instabilities of trapped metallic nanoparticles. However, the generation of the thermoelectric field relies on the thermophoresis of ionic species, thereby limiting its use to certain liquid environments. Furthermore, it is primarily a two-dimensional approach, while 3D manipulation can be achieved through incorporation of an optical fiber.

3.4 Optothermal manipulation with photophoresis

Since photophoretic force points from hot to cold, light-absorbing particles prefer to migrate to the low-intensity or even zero-intensity regions. Thus, optical engineering of the heating laser beam can lead to different functions. For instance, using a vortex beam[51] or a Gaussian beam by combination of the spherical aberration,[52] one can confine particles at the low-intensity regions of the laser beam for photophoretic trapping. More interestingly, photophoresis can be harnessed for optical pulling of light-absorbing particles when predominant absorption occurs at one side of the particles. [53–54] Shvedov *et al.* reported the transition from photophoretic repelling to photophoretic pulling of semitransparent particles when the heating laser is switched from radial polarization to azimuthal polarization.[53] Manipulation of colloidal particles in the air has interesting applications. For instance, Smalley *et al.* has recently demonstrated the photophoretic trapping of single cellulose particles for a volumetric display. The photophoretic trapping sites were created through combination of spherical and astigmatic aberrations. The trapped particle was then scanned at a high-speed and simultaneously illuminated by collinear red, green, and blue lasers for a color display (Fig. 9a).[55] This novel technique provides arbitrary, full-color 3D images which can be seen from most angles (Fig. 9b).

4. PERSPECTIVE

Optimization of light-controlled temperature gradients is the key to optothermal manipulation. Future development of this field relies on the rational management of optical heating. Specifically, any substrate with a high optothermal conversion efficiency and a low thermal conductivity is highly desired to improve the optothermal manipulation efficiency and to reduce optical power for non-invasive manipulation. There is also much room for optimization of the heating optics. For example, use of a femtosecond laser pulse for optical heating could limit both heat transfer and collective heating on the substrates, improving the temperature gradient for optothermal trapping.

The functionality of optothermal manipulation can be extended by multiple-field coupling. We have shown that coupling of light, temperature, and electric fields enables opto-thermoelectric manipulation. We expect that incorporation of a magnetic field into a light-controlled temperature field will enable opto-thermomagnetic manipulation. Examples include optical heating of ferromagnetic particles to around their Curie point, at which ferromagnetic materials lose their permanent magnetic properties. In addition, design of complex particles such as Janus particles with regions of different optical, thermal, electric or magnetic responses could provide new manipulation scenarios and functionalities.

One of the most promising applications of optothermal manipulation is the assembly of functional colloidal materials and devices. Practical applications of colloidal materials and devices depend on the development of scalable and versatile assembly techniques. Through versatile control of configurations and inter-particle interactions, optothermal manipulation techniques enable a wide range of functional colloidal devices such as colloidal waveguides, tunable lasers, and sensors.

Future use of optothermal techniques for non-invasive manipulation of biological objects will bring new revolutions in life sciences and early disease diagnostics. Recently, Reichl *et al.* demonstrated thermophoretic manipulation of molecules in living cells.[56] In contrast to electrophoresis where the electric field can be screened by the cell membrane and electrophoretic control can hardly function, opto-thermophoresis can be compatible with cellular environments. It should be noted that biological membranes significantly change across species and with environmental temperature, and pH, providing both opportunities and challenges for optothermal manipulation of biological objects. In all cases the temperature field should be carefully designed to avoid thermally-induced biological damage.

5. CONCLUDING REMARKS

Optothermal manipulation techniques, which exploit photon-phonon conversion and heat-directed migration, provide versatile control of diverse species such as colloidal particles, micelles, molecules, and living cells. Various approaches for optothermal manipulation of colloidal particles and living cells have been demonstrated through a combination of Marangoni convection, thermophoresis, thermoelectricity, and depletion attraction. In contrast to conventional optical tweezers, which often rely on optical gradient force generated with rigorous optics and a high-power laser, optothermal manipulation techniques use low-power and simple optics.

We anticipate that with their low-power, non-invasive and versatile manipulations of colloidal particles, living cells and molecules, optothermal manipulation techniques will not only accelerate progress in scientific research in colloidal sciences, life sciences, nanoscience and materials sciences, but also lead to new functional materials, nanomedicines and diagnostic tools. For example, the optothermal assembly of colloidal matter at single-particle resolution will provide a new platform for exploration of how matter organizes. Molecular manipulation across and inside living cells will also provide new insights into cellular drug delivery and intracellular biomolecular interactions.

Acknowledgments

The authors acknowledge the financial supports of the Beckman Young Investigator Program, the Army Research Office (W911NF-17-1-0561) and the National Institute of General Medical Sciences of the National Institutes of Health (DP2GM128446). We thank our students and collaborators for their tremendous contributions to our work featured in this account.

References

1. Grier DG. A revolution in optical manipulation. Nature. 2003; 424:810–816. [PubMed: 12917694]

2. Jauffred L, Richardson AC, Oddershede LB. Three-Dimensional Optical Control of Individual Quantum Dots. Nano Lett. 2008; 8:3376–3380. [PubMed: 18767883]
3. Hansen PM, Bhatia VK, Harrit N, Oddershede L. Expanding the Optical Trapping Range of Gold Nanoparticles. Nano Lett. 2005; 5:1937–1942. [PubMed: 16218713]
4. Babynina A, Fedoruk M, Kühler P, Meledin A, Döblinger M, Lohmüller T. Bending Gold Nanorods with Light. Nano Lett. 2016; 16:6485–6490. [PubMed: 27598653]
5. Grigorenko AN, Roberts NW, Dickinson MR, Zhang Y. Nanometric optical tweezers based on nanostructured substrates. Nat Photonics. 2008; 2:365–370.
6. Zheng Y, Ryan J, Hansen P, Cheng YT, Lu TJ, Hesselink L. Nano-Optical Conveyor Belt, Part II: Demonstration of Handoff Between Near-Field Optical Traps. Nano Lett. 2014; 14:2971–2976. [PubMed: 24807058]
7. Chiou PY, Ohta AT, Wu MC. Massively parallel manipulation of single cells and microparticles using optical images. Nature. 2005; 436:370–372. [PubMed: 16034413]
8. Piazza R, Parola A. Thermophoresis in colloidal suspensions. J Phys : Condens Matter. 2008; 20:153102.
9. Würger A. Thermal non-equilibrium transport in colloids. Rep Prog Phys. 2010; 73:126601.
10. Donner JS, Baffou G, McCloskey D, Quidant R. Plasmon-Assisted Optofluidics. ACS Nano. 2011; 5:5457–5462. [PubMed: 21657203]
11. Helden L, Eichhorn R, Bechinger C. Direct measurement of thermophoretic forces. Soft Matter. 2015; 11:2379–2386. [PubMed: 25673057]
12. Putnam SA, Cahill DG, Wong GCL. Temperature Dependence of Thermodiffusion in Aqueous Suspensions of Charged Nanoparticles. Langmuir. 2007; 23:9221–9228. [PubMed: 17655335]
13. Braibanti M, Vigolo D, Piazza R. Does Thermophoretic Mobility Depend on Particle Size? Phys Rev Lett. 2008; 100:108303. [PubMed: 18352238]
14. Würger A. Transport in Charged Colloids Driven by Thermoelectricity. Phys Rev Lett. 2008; 101:108302. [PubMed: 18851262]
15. Reichl M, Herzog M, Götz A, Braun D. Why Charged Molecules Move Across a Temperature Gradient: The Role of Electric Fields. Phys Rev Lett. 2014; 112:198101. [PubMed: 24877967]
16. Braun D, Libchaber A. Trapping of DNA by Thermophoretic Depletion and Convection. Phys Rev Lett. 2002; 89:188103. [PubMed: 12398641]
17. Duhr S, Braun D. Why molecules move along a temperature gradient. Proc Natl Acad Sci. 2006; 103:19678–19682. [PubMed: 17164337]
18. Jiang HR, Wada H, Yoshinaga N, Sano M. Manipulation of Colloids by a Nonequilibrium Depletion Force in a Temperature Gradient. Phys Rev Lett. 2009; 102:208301. [PubMed: 19519079]
19. Flores-Flores E, Torres-Hurtado SA, Páez R, Ruiz U, Beltrán-Pérez G, Neale SL, Ramirez-San-Juan JC, Ramos-García R. Trapping and manipulation of microparticles using laser-induced convection currents and photophoresis. Biomed Opt Express. 2015; 6:4079–4087. [PubMed: 26504655]
20. Piazza R, Guarino A. Soret Effect in Interacting Micellar Solutions. Phys Rev Lett. 2002; 88:208302. [PubMed: 12005610]
21. Iacopini S, Piazza R. Thermophoresis in protein solutions. Europhys Lett. 2003; 63:247.
22. Parola A, Piazza R. Particle thermophoresis in liquids. Eur Phys J E. 2004; 15:255–263. [PubMed: 15592765]
23. Duhr S, Braun D. Thermophoretic Depletion Follows Boltzmann Distribution. Phys Rev Lett. 2006; 96:168301. [PubMed: 16712279]
24. Edwards TD, Bevan MA. Depletion-Mediated Potentials and Phase Behavior for Micelles, Macromolecules, Nanoparticles, and Hydrogel Particles. Langmuir. 2012; 28:13816–13823. [PubMed: 22950666]
25. Vigolo D, Buzzaccaro S, Piazza R. Thermophoresis and Thermoelectricity in Surfactant Solutions. Langmuir. 2010; 26:7792–7801. [PubMed: 20146491]
26. Majee A, Würger A. Charging of Heated Colloidal Particles Using the Electrolyte Seebeck Effect. Phys Rev Lett. 2012; 108:118301. [PubMed: 22540514]

27. Yalamov YI, Kutukov VB, Shchukin ER. Theory of the photophoretic motion of the large-size volatile aerosol particle. J Colloid Interface Sci. 1976; 57:564–571.
28. Fang Z, Zhen YR, Neumann O, Polman A, García de Abajo FJ, Nordlander P, Halas NJ. Evolution of Light-Induced Vapor Generation at a Liquid-Immersed Metallic Nanoparticle. Nano Lett. 2013; 13:1736–1742. [PubMed: 23517407]
29. Baffou G, Polleux J, Rigneault H, Monneret S. Super-Heating and Micro-Bubble Generation around Plasmonic Nanoparticles under cw Illumination. J Phys Chem C. 2014; 118:4890–4898.
30. Zhao C, Xie Y, Mao Z, Zhao Y, Rufo J, Yang S, Guo F, Mai JD, Huang TJ. Theory and experiment on particle trapping and manipulation via optothermally generated bubbles. Lab Chip. 2014; 14:384–391. [PubMed: 24276624]
31. Villangca MJ, Palima D, Banas AR, Gluckstad J. Light-driven micro-tool equipped with a syringe function. Light Sci Appl. 2016; 5:e16148.
32. Lin L, Peng X, Mao Z, Li W, Yogeesh MN, Rajeeva BB, Perillo EP, Dunn AK, Akinwande D, Zheng Y. Bubble-Pen Lithography. Nano Lett. 2016; 16:701–708. [PubMed: 26678845]
33. Lukianova-Hleb E, Hu Y, Latterini L, Tarpani L, Lee S, Drezek RA, Hafner JH, Lapotko DO. Plasmonic Nanobubbles as Transient Vapor Nanobubbles Generated around Plasmonic Nanoparticles. ACS Nano. 2010; 4:2109–2123. [PubMed: 20307085]
34. Bangalore Rajeeva B, Lin L, Perillo EP, Peng X, Yu WW, Dunn A, Zheng Y. High-Resolution Bubble Printing of Quantum Dots. ACS Applied Materials & Interfaces. 2017; 9:16725–16733. [PubMed: 28452214]
35. Rajeeva BB, Alabandi MA, Lin L, Perillo EP, Dunn AK, Zheng Y. Patterning and Fluorescence Tuning of Quantum Dots with Haptic-Interfaced Bubble Printing. Journal of Materials Chemistry C. 2017; 5:5693–5699. [PubMed: 29599983]
36. Urban AS, Lutich AA, Stefani FD, Feldmann J. Laser Printing Single Gold Nanoparticles. Nano Lett. 2010; 10:4794–4798. [PubMed: 20957994]
37. Nedev S, Urban AS, Lutich AA, Feldmann J. Optical Force Stamping Lithography. Nano Lett. 2011; 11:5066–5070. [PubMed: 21992538]
38. Gargiulo J, Violi IL, Cerrotta S, Chvátal L, Cortes E, Perassi EM, Diaz F, Zemanek P, Stefani FD. Accuracy and Mechanistic Details of Optical Printing of Single Au and Ag Nanoparticles. ACS Nano. 2017
39. Walker D, Singh DP, Fischer P. Capture of 2D Microparticle Arrays via a UV-Triggered Thiol-yne “Click” Reaction. Adv Mater. 2016; 28:9846–9850. [PubMed: 27717081]
40. Braun M, Cichos F. Optically Controlled Thermophoretic Trapping of Single Nano-Objects. ACS Nano. 2013; 7:11200–11208. [PubMed: 24215133]
41. Braun M, Wurger A, Cichos F. Trapping of single nano-objects in dynamic temperature fields. Phys Chem Chem Phys. 2014; 16:15207–15213. [PubMed: 24939651]
42. Lin L, Peng X, Mao Z, Wei X, Xie C, Zheng Y. Interfacial-entropy-driven thermophoretic tweezers. Lab Chip. 2017; 17:3061–3070. [PubMed: 28805878]
43. Lin L, Peng X, Wei X, Mao Z, Xie C, Zheng Y. Thermophoretic Tweezers for Low-Power and Versatile Manipulation of Biological Cells. ACS Nano. 2017; 11:3147–3154. [PubMed: 28230355]
44. Wu MC. Optoelectronic tweezers. Nat Photonics. 2011; 5:322–324.
45. Lin L, Wang M, Peng X, Lissek EN, Mao Z, Scarabelli L, Adkins E, Coskun S, Unalan HE, Korgel BA, Liz-Marzan LM, Florin EL, Zheng Y. Opto-thermoelectric nanotweezers. Nat Photonics. 2018; 12:195–201. [PubMed: 29785202]
46. Rings D, Schachoff R, Selmke M, Cichos F, Kroy K. Hot Brownian Motion. Phys Rev Lett. 2010; 105:090604. [PubMed: 20868149]
47. Lin L, Peng X, Wang M, Scarabelli L, Mao Z, Liz-Marzán LM, Becker MF, Zheng Y. Light-Directed Reversible Assembly of Plasmonic Nanoparticles Using Plasmon-Enhanced Thermophoresis. ACS Nano. 2016; 10:9659–9668.
48. Lin L, Zhang J, Peng X, Wu Z, Coughlan ACH, Mao Z, Bevan MA, Zheng Y. Opto-thermophoretic assembly of colloidal matter. Science Advances. 2017; 3:E1700458. [PubMed: 28913423]
49. Iracki TD, Beltran-Villegas DJ, Eichmann SL, Bevan MA. Charged Micelle Depletion Attraction and Interfacial Colloidal Phase Behavior. Langmuir. 2010; 26:18710–18717. [PubMed: 21077612]

50. Lin L, Peng X, Zheng Y. Reconfigurable opto-thermoelectric printing of colloidal particles. Chem Commun. 2017; 53:7357–7360.
51. Shvedov VG, Rode AV, Izdebskaya YV, Desyatnikov AS, Krolikowski W, Kivshar YS. Giant Optical Manipulation. Phys Rev Lett. 2010; 105:118103. [PubMed: 20867612]
52. Zhang P, Zhang Z, Prakash J, Huang S, Hernandez D, Salazar M, Christodoulides DN, Chen Z. Trapping and transporting aerosols with a single optical bottle beam generated by moiré techniques. Opt Lett. 2011; 36:1491–1493. [PubMed: 21499400]
53. Shvedov V, Davoyan AR, Hnatovsky C, Engheta N, Krolikowski W. A long-range polarization-controlled optical tractor beam. Nat Photon. 2014; 8:846–850.
54. Lu J, Yang H, Zhou L, Yang Y, Luo S, Li Q, Qiu M. Light-Induced Pulling and Pushing by the Synergic Effect of Optical Force and Photophoretic Force. Phys Rev Lett. 2017; 118:043601. [PubMed: 28186804]
55. Smalley DE, Nygaard E, Squire K, Van Wagoner J, Rasmussen J, Gneiting S, Qaderi K, Goodsell J, Rogers W, Lindsey M, Costner K, Monk A, Pearson M, Haymore B, Peatross J. A photophoretic-trap volumetric display. Nature. 2018; 553:486. [PubMed: 29368704]
56. Reichl MR, Braun D. Thermophoretic Manipulation of Molecules inside Living Cells. J Am Chem Soc. 2014; 136:15955–15960. [PubMed: 25171388]

Biographies

Linhan Lin is a research associate in Yuebing Zheng’s group. He received both his B.S. and Ph.D. degrees in Materials Science and Engineering from Tsinghua University.

Eric H. Hill is a postdoctoral researcher in Yuebing Zheng’s group. He received his B.S. in Chemistry from Southern Oregon University, and his Ph.D. in Nanoscience and Microsystems Engineering from the University of New Mexico.

Xiaolei Peng is a Ph. D. candidate in Yuebing Zheng’s group. He received his B.S. in Physics from Peking University.

Yuebing Zheng is an assistant professor of Mechanical Engineering and Materials Science & Engineering at the University of Texas at Austin. He received his Ph.D. in Engineering Science and Mechanics from The Pennsylvania State University in 2010. He was a postdoctoral researcher at the University of California, Los Angeles from 2010 to 2013. His research group engage in interdisciplinary research to innovate optical nanotechnologies in health, energy, manufacturing, and national security. He has been awarded the NIH Director’s New Innovator Award, the NASA Early Career Faculty Award, the ONR Young Investigator Award, and the Beckman Young Investigator Award.

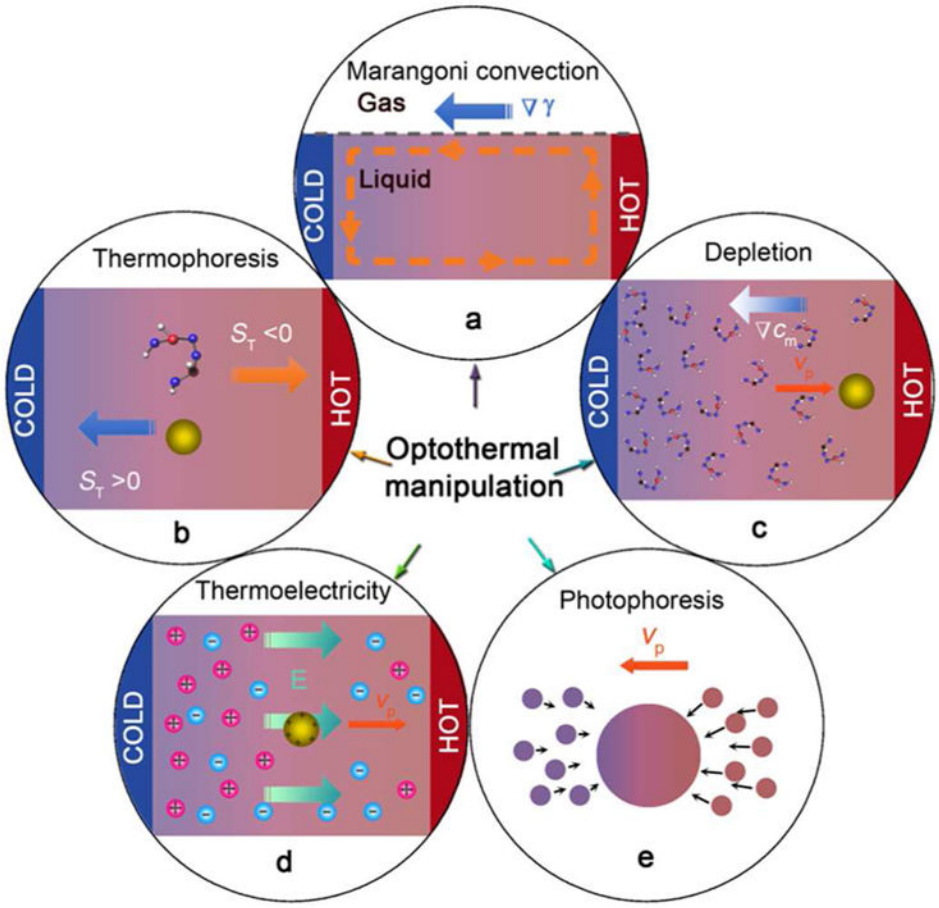

Figure 1.

(a) Schematic illustration of theoretical models for the various optothermal processes: (a) Marangoni convection at the liquid-gas interface, (b) thermophoresis, (c) depletion, (d) thermoelectricity, and (e) photophoresis.

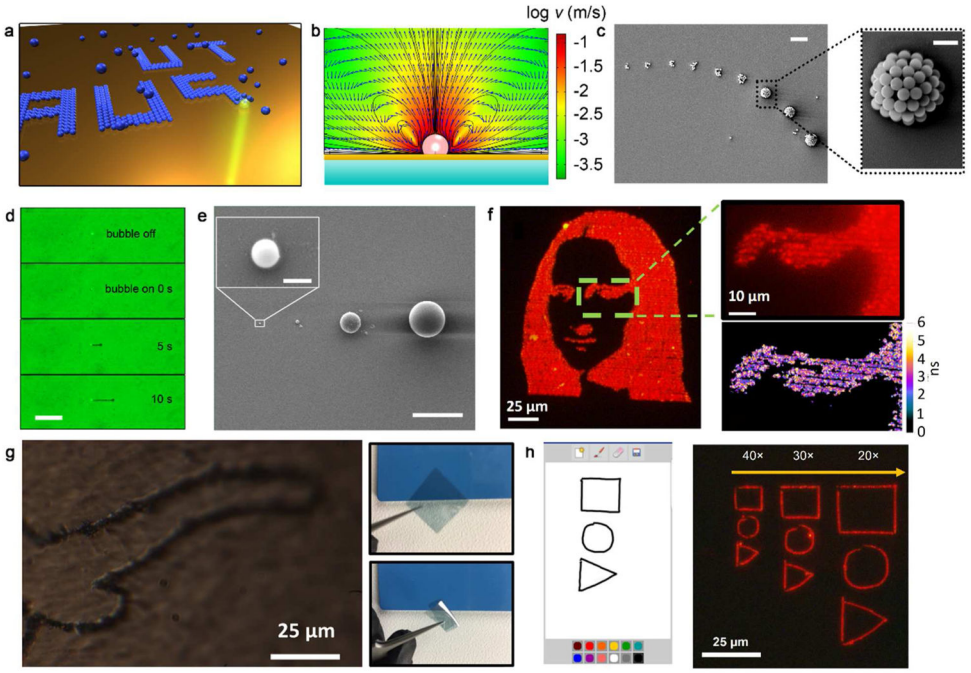

Figure 2.

Bubble-printing of colloidal particles. (a) Schematic illustration of bubble-pen lithography (BPL); (b) Simulated Marangoni convection around a 1 μm bubble; (c) Printed 500 nm PS beads at different power; Scale bar: 5 μm (left) and 1 μm (right). (d) Continuous writing with BPL; Scale bar: 50 μm (e) Single-particle printing; Scale bar: 10 μm (bottom) and 500 nm (top).[32] Adapted with permission from ref 32. Copyright 2016 American Chemical Society. (f) "Mona Lisa" pattern of quantum dots with fluorescence lifetime mapping; (g) Printing of quantum dots on a flexible substrate.[34] Adapted with permission from ref 34. Copyright 2017 American Chemical Society. (h) Haptic interface for bubble printing at different downscaling factors.[35] Adapted with permission from ref 35. Copyright 2017 The Royal Society of Chemistry.

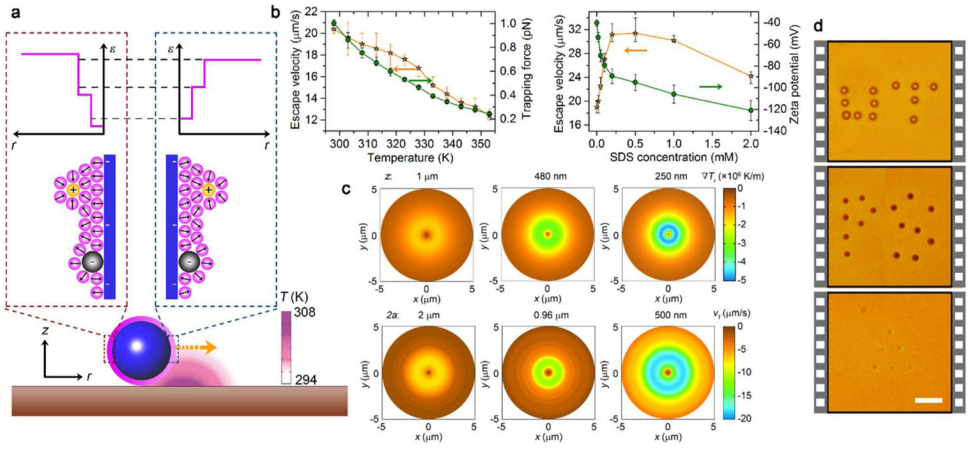

Figure 3.

Opto-thermophoretic tweezers for manipulation of colloidal particles. (a) Schematic illustration of working principle of the tweezers; (b) Tunable trapping capability depending on solution temperature and SDS concentration; (c) Verification of the thermophoretic migration of particles by the proportional relationship between trapping velocity and temperature gradient; (d) Parallel trapping of colloidal particles of different sizes.[42] Scale bar: 10 μm. Adapted with permission from ref 42. Copyright 2017 The Royal Society of Chemistry.

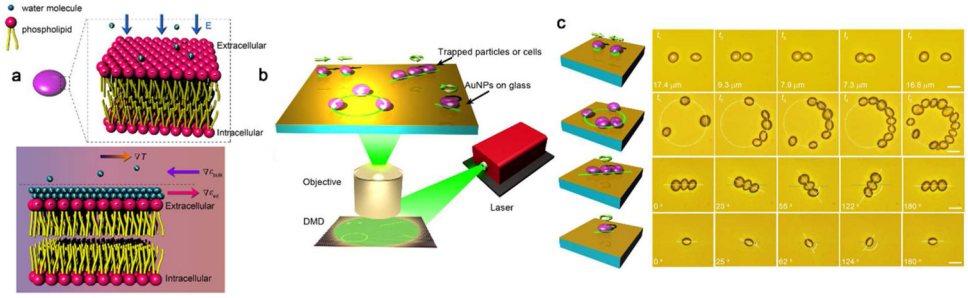

Figure 4.

Opto-thermophoretic tweezers for manipulation of biological cells. (a) Schematic illustration of the working principle; (b) Optical setup of the tweezers; (c) Versatile manipulation of yeast cells.[43] Scale bar: 10 μm. Adapted with permission from ref 43. Copyright 2017 American Chemical Society.

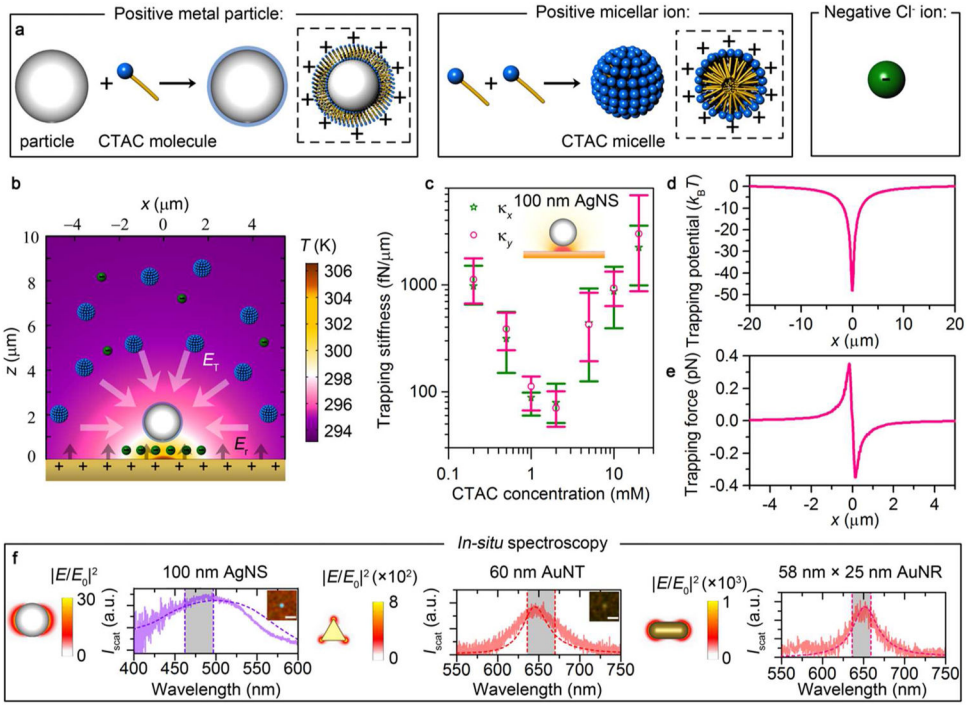

Figure 5.

Opto-thermoelectric trapping of metal nanoparticles. (a) Components of the colloidal solution; (b) Schematic illustration of working principle of the tweezers; (c) CTAC-dependent trapping stiffness, (d) trapping potential and (e) trapping force of single 100 nm AgNSs. (f) *In-situ* dark-field optical spectroscopy of trapped single metal nanoparticles along with simulated spectra.[45] Scale bars: 2 μm. Adapted with permission from ref 45. Copyright 2018 Springer Nature.

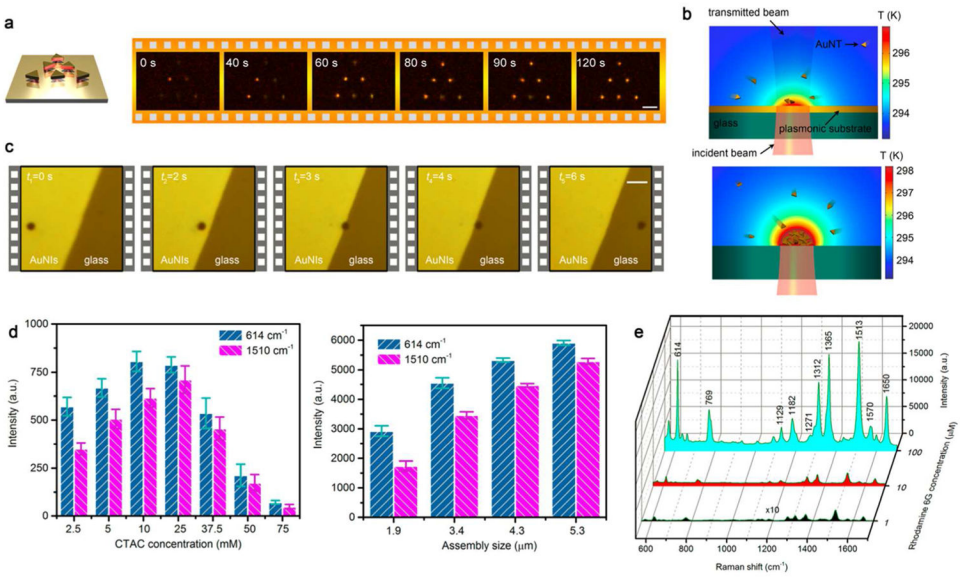

Figure 6.

Opto-thermoelectric manipulation of multiple metal nanoparticles. (a) Parallel trapping of six 150 nm gold nanotriangles (AuNTs).[45] Scale bars: 5 μm. Adapted with permission from ref 45. Copyright 2018 Springer Nature; (b) Simulated temperature fields for plasmonic substrate (top panel) and particle assembly (bottom panel); (c) Transport of particle assembly from plasmonic to non-plasmonic substrate; Scale bar: 10 μm. (d) SERS sensitivity of rhodamine 6G as a function of CTAC concentration and assembly size; (e) Detection limit of rhodamine 6G based on AgNS assemblies.[47] Adapted with permission from ref 47. Copyright 2016 American Chemical Society.

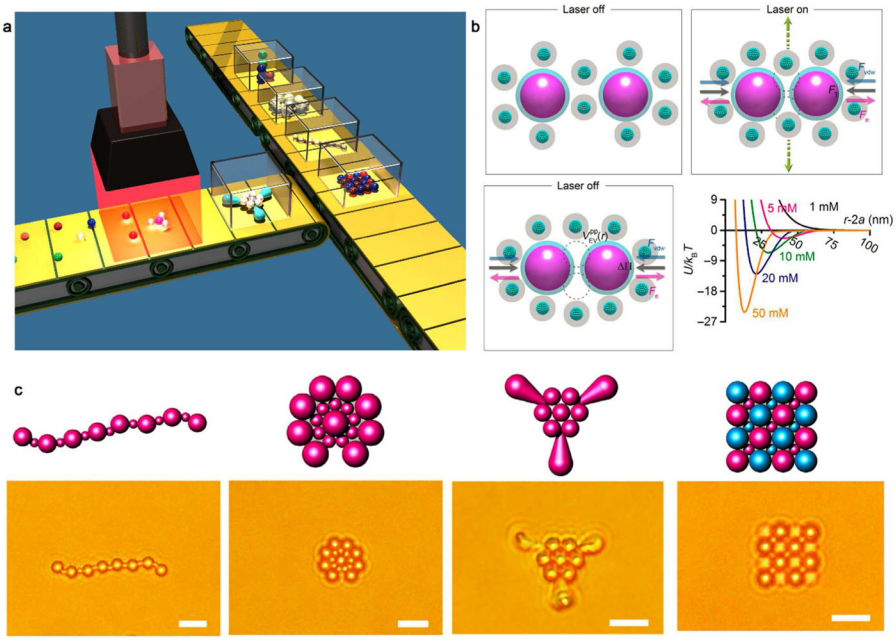

Figure 7.

Optothermal assembly of particles into colloidal matter. (a) Illustration of the assembly process; (b) Illustration of inter-particle bonding and dependence of its potential on CTAC concentration; (c) Diverse types of colloidal matter assembled optothermally.[48] Scale bar: 5 μm. Adapted with permission from ref 48. Copyright 2017 American Association for the Advancement of Science.

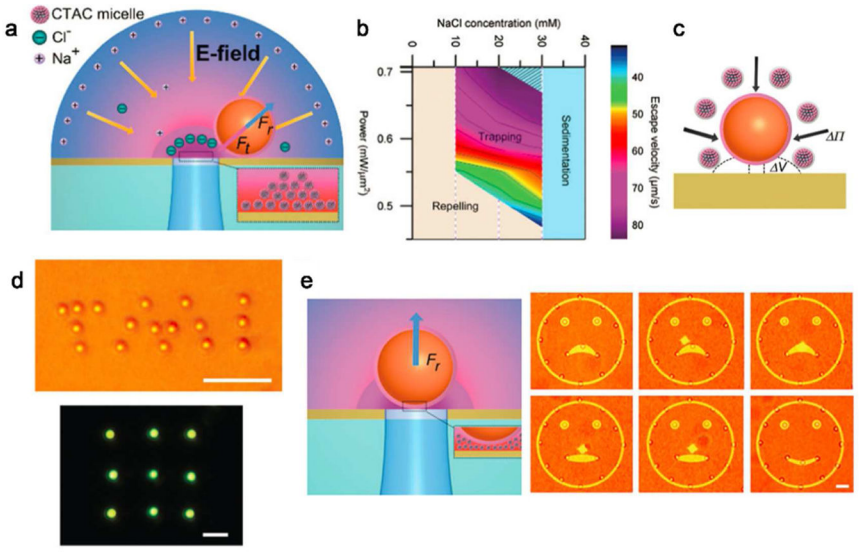

Figure 8.

Reconfigurable opto-thermoelectric printing of colloidal particles on the substrates. (a) Working principle of reconfigurable printing, F_t and F_r are the trapping force and repelling force on the particle, respectively; (b) Phase diagram showing different particle-manipulation regimes; (c) Micelle-mediated depletion attraction between a particle and a substrate; (d) Printed “TMI” pattern of 1 μm PS beads and 3-by-3 array of 500 nm PS beads; Scale bars: 10 μm (top) and 5 μm (bottom); (e) Releasing and reprinting of a targeted colloidal particle.50 Adapted with permission from ref 50. Copyright 2017 The Royal Society of Chemistry.

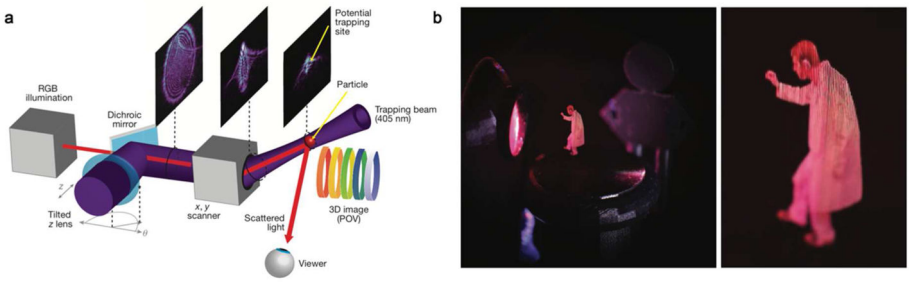

Figure 9.

Photophoretic manipulation of particles. (a) Optical setup and (b) demonstrated 3D optical images of optical trap display.[55] Adapted with permission from ref 55. Copyright 2018 Springer Nature.